Cell Tissue Res (2002) 307:371–379
DOI 10.1007/s00441-002-0517-z

REGULAR ARTICLE

Xudong Qiu · Kurt A.J. Vanhoutte
Doekele G. Stavenga · Kentaro Arikawa

Ommatidial heterogeneity in the compound eye of the male small white butterfly, Pieris rapae *crucivora*

Received: 27 August 2001 / Accepted: 9 January 2002 / Published online: 23 February 2002

Abstract The ommatidia in the ventral two-thirds of the compound eye of male *Pieris rapae crucivora* are not uniform. Each ommatidium contains nine photoreceptor cells. Four cells (R1–4) form the distal two-thirds of the rhabdom, four cells (R5–8) approximately occupy the proximal one-third of the rhabdom, and the ninth cell (R9) takes up a minor basal part of the rhabdom. The R5–8 photoreceptor cells contain clusters of reddish pigment adjacent to the rhabdom. From the position of the pigment clusters, three types of ommatidia can be identified: the trapezoidal (type I), square (type II), and rectangular type (type III). Microspectrophotometry with an epi-illumination microscope has revealed that the reflectance spectra of type I and type III ommatidia peak at 635 nm and those of type II ommatidia peak at 675 nm. The bandwith of the reflectance spectra is 40–50 nm. Type II ommatidia strongly fluoresce under ultra-violet and violet epi-illumination. The three types of ommatidia are randomly distributed. The ommatidial heterogeneity is presumably crucial for color discrimination.

Keywords Compound eye · Retina · Photoreceptor · Rhabdom · Color vision · Tapetum ·*Pieris rapae crucivora* (Insecta)

Introduction

Insect eyes consist of numerous, anatomically identical units, the ommatidia, which are often very regularly arranged, in a crystalline facet lattice. Recent research on butterflies, specifically the Japanese yellow swallowtail, *Papilio xuthus*, has shown that the ommatidial lattice is not a perfect repetitive structure and, indeed, consists of three classes of randomly arranged ommatidia. The different types of ommatidia are histologically discriminable by the color of the pigments (red or yellow) around the rhabdom. The pigments function as spectral filters for the photoreceptor cells forming the proximal part of the rhabdom (Arikawa et al. 1999b). Some of the ommatidia fluoresce strongly under ultra-violet (UV) epi-illumination, probably because of 3-hydroxyretinol, which is located distally in the ommatidia, and which functions as a UV-absorbing filter (Arikawa and Stavenga 1997; Arikawa et al. 1999a). Combined electrophysiological and molecular biological investigations have identified the unique combination of spectral receptors contained in each of the three types of ommatidia (Kitamoto et al. 2000). The results indicate that the random meshwork of the three ommatidial classes of *Papilio xuthus* is crucial for mediating color vision (Kinoshita et al. 1999).

This has raised the question of whether other butterflies share the arrangement of photoreceptors found in the compound eye of *Papilio*. It is known that all butterflies, except for the Papilionidae, possess a tapetum, a mirror-like structure at the base of each ommatidium. The tapetum is a tracheole folded into a stack of layers, alternately consisting of air and cytoplasm, thus creating an interference reflection filter. Incident light that has propagated along the light-guiding rhabdom is reflected and leaves the eye again, visible as the so-called butterfly eyeshine. A survey of several butterfly species from different families has shown that the eyeshine from adjacent ommatidia is variable, strongly suggesting that the spectral heterogeneity of ommatidia is a general characteristic of butterfly eyes (Bernard and Miller 1970; Stavenga et al. 2001; Stavenga 2002).

Of butterflies with a tapetum, the visual characteristics of the Pieridae have been intensely investigated in the last few decades (Obara and Hidaka 1968; Ribi 1978,

This work was supported by Research Grants from the Ministry of Education, Science, and Culture of Japan to K.A.

X. Qiu · K. Arikawa (✉)
Graduate School of Integrated Science,
Yokohama City University, 22-2 Seto, Kanazawa-ku,
Yokohama 236-0027, Japan
e-mail: arikawa@yokohama-cu.ac.jp
Tel.: +81-45-7872212, Fax: +81-45-7872212

K.A.J. Vanhoutte · D.G. Stavenga
Department of Neurobiophysics, University of Groningen,
Groningen, The Netherlands

1979a, 1979b, 1980; Kolb 1978; Scherer and Kolb 1987; Shimohigashi and Tominaga 1991; Goulson and Cory 1993; Kandori and Ohsaki 1996). The study of Shimohigashi and Tominaga (1991) is of specific interest, as it shows that the compound eye of the small white, *Pieris rapae*, contains at least five different classes of spectral receptors, similar to those of *Papilio xuthus* (Arikawa et al. 1987). However, so far, the question of ommatidial heterogeneity has not been addressed in the Pieridae. Here, we present the first detailed study of the ommatidial structure in male *Pieris rapae*, by combining light- and electron-microscopic histology with in vivo epi-illumination microscopy and microspectrophotometry. We focus on the ventral two-thirds of the compound eye (hereafter referred to as the ventral eye region), in which Ribi (1979a) has demonstrated that the ommatidia are pigmented red. We conclude that three distinct different types of ommatidia exist in this eye region.

Materials and methods

Animals

We used spring-form males of *Pieris rapae crucivora* BOISDUVAL. The butterflies were taken from a laboratory stock derived from eggs laid by females caught in the field. The hatched larvae were reared on fresh kale leaves at 19°C under a light regime of 8 h light: 16 h dark. The pupae were stored at 4°C for at least 3 months and then allowed to emerge at 25°C prior to experimentation. The adults were used within 4 days after emergence.

Epi-illumination microscopy

The spatial arrangement of the different ommatidial types was investigated with a specially constructed epi-illumination light microscope by using a large-aperture microscope objective (Leitz LM 32, NA 0.6; Stavenga 2002). The reflection of monochromatic light (610 and 670 nm) and the fluorescence induced by broadband violet light (50 W Hg-lamp and Schott UG1 filter) were photographed with a Kodak DC120 digital camera.

The optical characteristics of the ommatidia were furthermore investigated with an epi-fluorescence microscope (BX-60, Olympus) equipped with a cooled charge-coupled device camera (CoolSnap, Olympus). We recorded the autofluorescence of the *Pieris* eye under both UV (with the U-MNU mirror unit, Olympus) and blue-violet (with the U-MNBV mirror unit, Olympus) epi-illumination. To correlate the results of fluorescence and pigmentation, we first injected the fluorescing dye Alexafluor 568 into a single photoreceptor and then identified the ommatidium containing the impaled photoreceptor under green excitation light (with the U-MWIG mirror unit, Olympus). We photographed the blue-violet-induced fluorescence from the same region and processed the eye for light-microscopic histology (see below). We thus identified the region in histological sections by using the stained photoreceptor as the reference.

Microspectrophotometry

The reflectance spectra of single ommatidia were measured with a microspectrophotometer constructed from an epi-illumination microscope (Leitz Ortholux) and a photodiode-array spectrophotometer (Avantes SD2000). Tapetal reflection resulting from illumination with a broadband white (150 W Xe) light source was measured from a single facet by adjusting a diaphragm in front of the spectrophotometer.

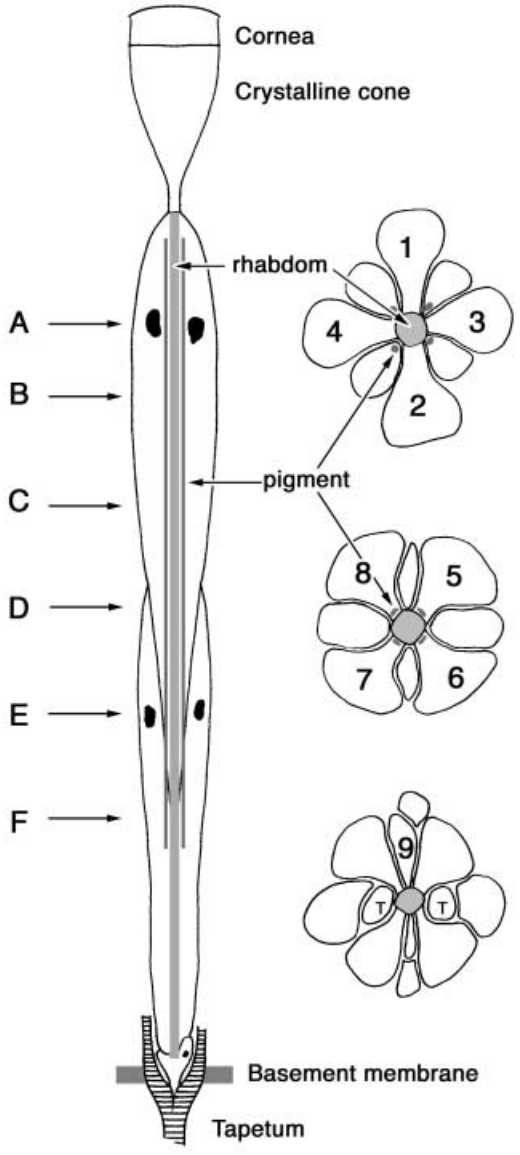

Fig. 1 Schematic drawing of a *Pieris rapae* ommatidium (*T* tapetum). A longitudinal view (*left*) and transverse view at three different levels (*right*). *Letters left* indicate the levels at which the micrographs in Fig. 5 were taken

The measured reflectance spectra can be formally interpreted by taking into account that light emerging from an ommatidium has traveled twice through the length of the rhabdom, having been reflected at the tapetum. The rhabdom transmittance is affected by two components; transmitted light is absorbed first by the visual pigments in the rhabdom interior and second by the screening pigments in the exterior medium surrounding the rhabdom.

Histology

For histological observation, we made semi-thin and ultra-thin sections of plastic-embedded compound eyes. Eyes were isolated, immediately immersed in 2% glutaraldehyde and 2% paraformaldehyde in 0.1 M sodium cacodylate buffer (pH 7.3, CB), and prefixed for 30 min at room temperature. After a 5-min wash with 0.1 M CB, the eyes were post-fixed in 2% OsO_4 in 0.1 M CB for 2 h at room temperature. The osmicated eyes were then dehydrated in a graded series of ethanol, infiltrated with propylene oxide, and embedded in Epon.

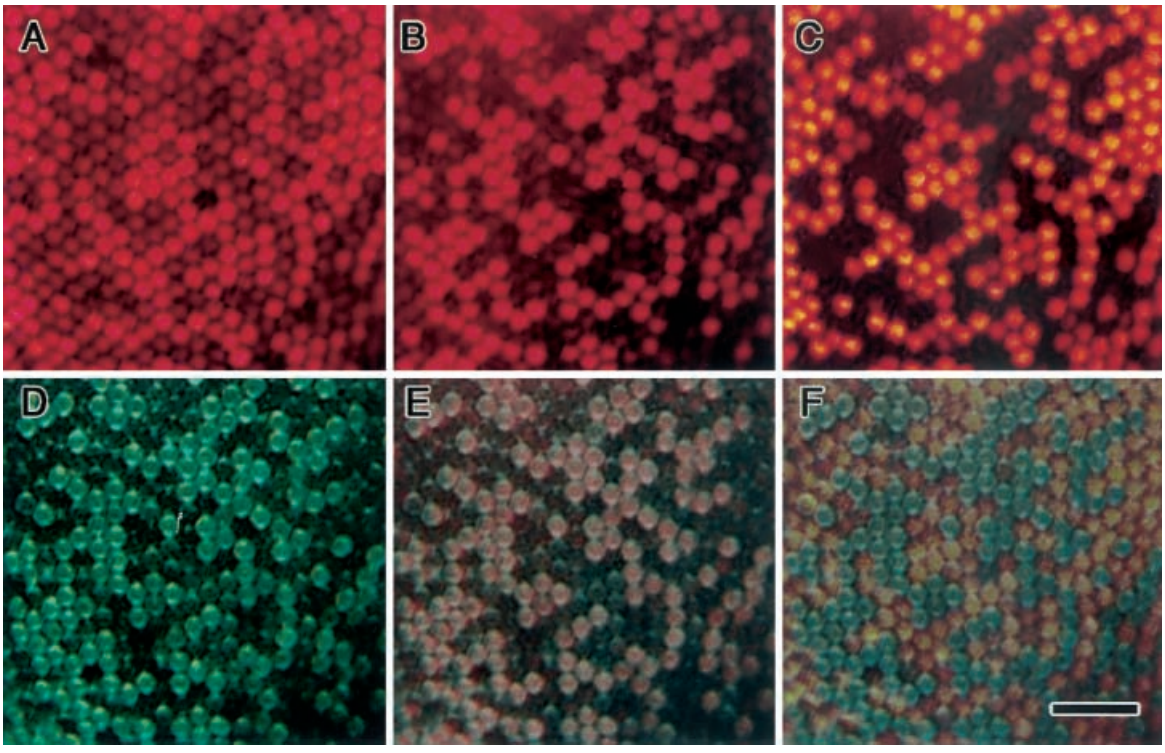

Fig. 2 Tapetal reflection with white (**A**), 670 nm (**B**), and 610 nm light (**C**), and fluorescence induced by blue-violet light (**D**) from the same area of a male *Pieris* eye. **E** Superposition of **B** (670 nm) and **D** (fluorescence). **F** Superposition of **C** (610 nm) and **D** (fluorescence). *Bar* 100 µm

For light microscopy, we made semi-thin (2 µm) sections. We examined the sections by regular transmission microscopy with no staining. For electron microscopy, we prepared ultrathin sections double-stained with 1% uranyl acetate in 50% ethanol and 0.1% lead citrate in distilled water, and observed them with a transmission electron microscope (JEM 1200EX).

Results

General morphology

The compound eye of the small white, *Pieris rapae*, is of a typical apposition type. The general histology has been described by Ribi (1978) and is therefore not repeated here in detail. The structure of the ommatidia is diagrammatically shown in Fig. 1. In the frontal-lateral looking part of the ventral region, the thickness of the dioptric apparatus (corneal lens and crystalline cone) is about 80 µm, and the photoreceptor layer measures about 400 µm. The total length of the ommatidium, from the corneal surface to the basement membrane, is hence about 480 µm. The diameter of the corneal facet lens is about 22 µm.

The rhabdom is composed of the rhabdomeres of nine photoreceptor cells, R1–9 (Ribi 1978). The photoreceptors R1–4 form the distal two-thirds of the rhabdom and are therefore called distal photoreceptors; the cell bodies of R1 and R2 are located along the dorso-ventral (or vertical) eye axis, and those of R3 and R4 are oriented along the horizontal axis. The proximal photoreceptors, R5–8, form the rhabdom in the proximal one-third; the cell bodies of R5–8 are arranged diagonally in the proximal tier of the ommatidium. A bi-lobed photoreceptor, R9, contributes a small basal part of the rhabdom, immediately distal to the basement membrane. Near the basement membrane, a tracheole creates the reflecting tapetum.

Tapetal reflection and ommatidial fluorescence

Epi-illumination with white light demonstrates that all ommatidia in the ventral region of the *Pieris* eye exhibit a red reflection with variable intensity (Fig. 2A). Monochromatic illumination with 670 nm (Fig. 2B) and 610 nm (Fig. 2C) indicates that there are two separate sets of reflecting ommatidia.

Epi-illumination fluorescence microscopy has revealed that, under violet excitation, a distinct set of ommatidia strongly fluoresces, and that the fluorescence of the other ommatidia is minor (Fig. 2D). The strongly fluorescing ommatidia also fluoresce under UV excitation (see below). Superimposing the fluorescence (Fig. 2D) and the 670 nm reflection micrographs (Fig. 2B) establishes that the fluorescing ommatidia reflect predominantly deep-red (670 nm) light (Fig. 2E). The minor fluorescing ommatidia are identical to those reflecting red (610 nm) light (Fig. 2F).

The reflection intensities vary somewhat within each ommatidial class (Fig. 2B, C). Reflectance spectra measured from individual ommatidia (Fig. 3) show that the spectra can be grouped into two separate spectral classes,

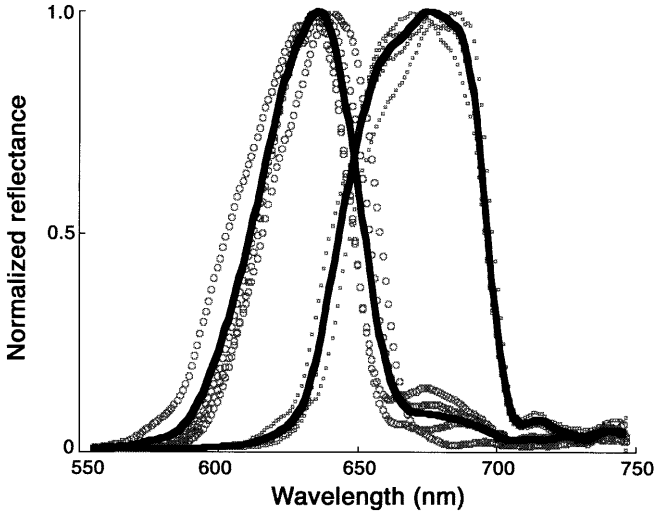

Fig. 3 Reflectance spectra measured from single ommatidia of a male *Pieris rapae*. The spectra, obtained by adjusting the measuring diaphragm at individual facets, fall in two classes, pale-red and deep-red, peaking at ca. 635 and 675 nm, respectively. Of each class, four spectra are shown; *large symbols* vs *small symbols* (*bold lines* average of the four spectra of each class, normalized at their peak value)

peaking at 635±5 nm and 675±5 nm, respectively. The spectra are narrow, with a half bandwidth of 40–50 nm. The variation in the reflectance spectra, notably in the long-wavelength tail of the pale-red-reflecting ommatidia, causes the variability in the reflection intensities at 670 nm in the micrographs in Fig. 2B.

To interpret the reflectance spectra, it is important to realize that the ommatidial reflections result from incident light that propagates down through the rhabdom, that is then reflected by the tapetum, and that subsequently travels back again through the rhabdom. The measured reflectance spectra thus are not only determined by the reflectance spectrum of the tapetum, but also by both the absorption by the visual pigments inside the light-guiding rhabdom and the screening pigments in the rhabdom boundary layer (Ribi 1978). The absorption by the visual pigments is negligible compared with that absorbed by the screening pigments in the long-wavelength range in Fig. 3.

The reflectance spectra in Fig. 3 show that the two classes of ommatidia in male *Pieris rapae* differ in tapetum and/or pigments. Histology substantiates this view. Figure 4 demonstrates that the fluorescing ommatidia correspond to a specific type of ommatidia identifiable by histology. To correlate the fluorescence and histology, we first injected Alexafluor 568 into a single photoreceptor. We then identified the ommatidium containing the stained photoreceptor under green epi-illumination (Fig. 4A). We also photographed the UV-induced and blue-violet-induced fluorescence of the same region to identify the fluorescing ommatidia (Fig. 4B, C; see also Fig. 2D). Ommatidia labeled with Alexafluor 568 emitted a slightly reddish fluorescence under UV epi-illumination (Fig. 4B, arrow). We further processed the eye for light-microscopic histology and then localized the Alexafluor-568-injected photoreceptor in a transverse section (Fig. 4D, E).

Proximally in the retina, all ommatidia have four clusters of screening pigment adjacent to the rhabdom. The pigment in the fluorescing ommatidia is deep-red and that in the non-fluorescing ommatidia is pale-red. The four deep-red clusters in the fluorescing ommatidia are arranged in a square pattern, whereas the arrangement of the pale-red clusters in the non-fluorescing ommatidia is less well defined.

Pigmentation

The pigmentation patterns have been investigated into more detail. Figure 5A–F shows a series of light-microscopical sections (from distal to proximal) of a central region of the *Pieris* compound eye. The four circles in each micrograph indicate the same set of ommatidia. The arrows in Fig. 5A, E indicate nuclei of a distal and a proximal photoreceptor, respectively (cf. Fig. 1).

For clarity, we will start from Fig. 5D, which is a transverse section at the depth of 260 µm from the corneal surface. Four spots surround the rhabdom, in the center of each ommatidium (arrowheads). These are the clusters of pigment granules in the proximal photoreceptor cells, R5–8. The clusters are arranged in three different patterns, indicating three types (instead of two types as identified in epi-illumination microscopy, see Fig. 2) of ommatidia: the pigment clusters (Fig. 5D) are arranged in a trapezoidal (type I, solid circles), square (type II, broken circle), and rectangular (type III, dotted circle) pattern, respectively. Type I has two subtypes: a trapezoid with a short upper side (middle circle) and a trapezoid with a long upper side (left circle).

The distal photoreceptors, R1–4, are also pigmented. In type I ommatidia, large dense pigment clusters occur in the distal part of R3 and R4 (Fig. 5A, arrowheads). In addition, a pigment cluster of lower density exists in the cell body of either R1 or R2 (white arrowheads in Fig. 5B). The pigmented R1 (or R2) forms the long side of the trapezoid in the middle layer (white arrowheads in Fig. 5E). The pigmentation in the distal photoreceptors (R1–4) disappears at a depth of 260 µm. The pigmentation of R5–8 emerges at about 180 µm (Fig. 5B) and disappears at about 360 µm.

The distal pigmentation of type II ommatidia is clearly different from that of the two other types. R1–4 photoreceptors have little pigmentation in the distal layer. On the other hand, the pigmentation of R5–8 photoreceptors emerges at 140 µm and is quite dense at 180 µm (Fig. 5B). The pigmentation of R5–8 in the distal region is not particularly clear in types I and III.

The distal pigmentation in type III ommatidia is similar to that in type I. Type III lacks the pigment clusters of lower density in photoreceptors R1 or R2.

We counted the numbers of the three types of ommatidia in eight micrographs of transverse sections taken

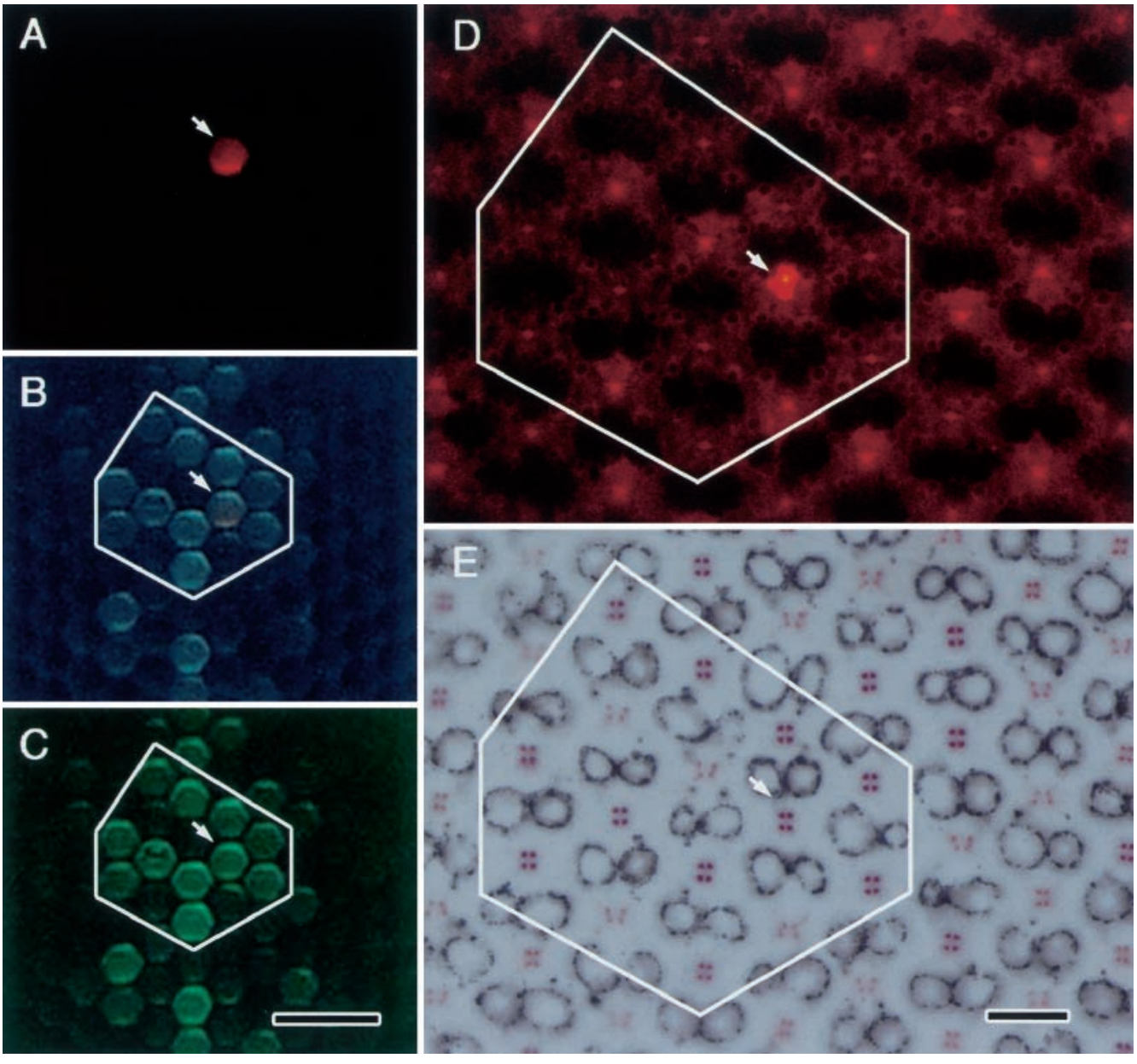

Fig. 4A–E Relationship between fluorescence and ommatidial histology in male *Pieris rapae* (*white polygons* identical sets of ommatidia). An ommatidium containing an Alexafluor-568-injected photoreceptor is identified in the intact eye by green-induced *red* fluorescence (**A**, *arrow*). Fluorescence of the same eye region under UV (**B**) and blue-violet (**C**) epi-illumination. The *reddish* fluorescence of Alexafluor 568 is also detectable in **B**, but not in **C** (*arrows*). Transverse sections of the same region under green epi-illumination (**D**) and regular transmission illumination (**E**). *Arrows* in **D** and **E** indicate the photoreceptor cell filled with Alexafluor 568. The fluorescing ommatidia contain, in addition to the fluorescing pigment, clusters of *deep-red* pigment. The clusters are arranged in a square pattern. The non-fluorescing ommatidia contain a *lighter red* pigment, also in four clusters, but in different patterns. The *black* pigment between the ommatidia marks the secondary pigment cells. *Bar* 50 µm (**A–C**), 10 µm (**D, E**)

from the middle part of the eye of eight individuals. Among 1009 ommatidia, type I occupied about a half (subtype 1=255, subtype 2=244, total 499 or 49.5%). Type II and III ommatidia numbered 291 (28.8%) and 219 (21.7%), respectively. To determine whether the array of the different types of ommatidia had any regularity, we counted the frequency of transition, e.g., from type I to type II or from type I to type III, along the three axes of the hexagonal lattice. We calculated the probability of transition assuming that the ommatidial distribution is random, i.e., the type of the neighbors solely depended on the absolute frequency of each ommatidial type. Comparison with the actual count and the calculated probablility revealed that they were not statistically different: the distribution was random, at least in the ventral eye region (eight micrographs yielded Chi-square=10.37, d.f.=18, $P>0.90$).

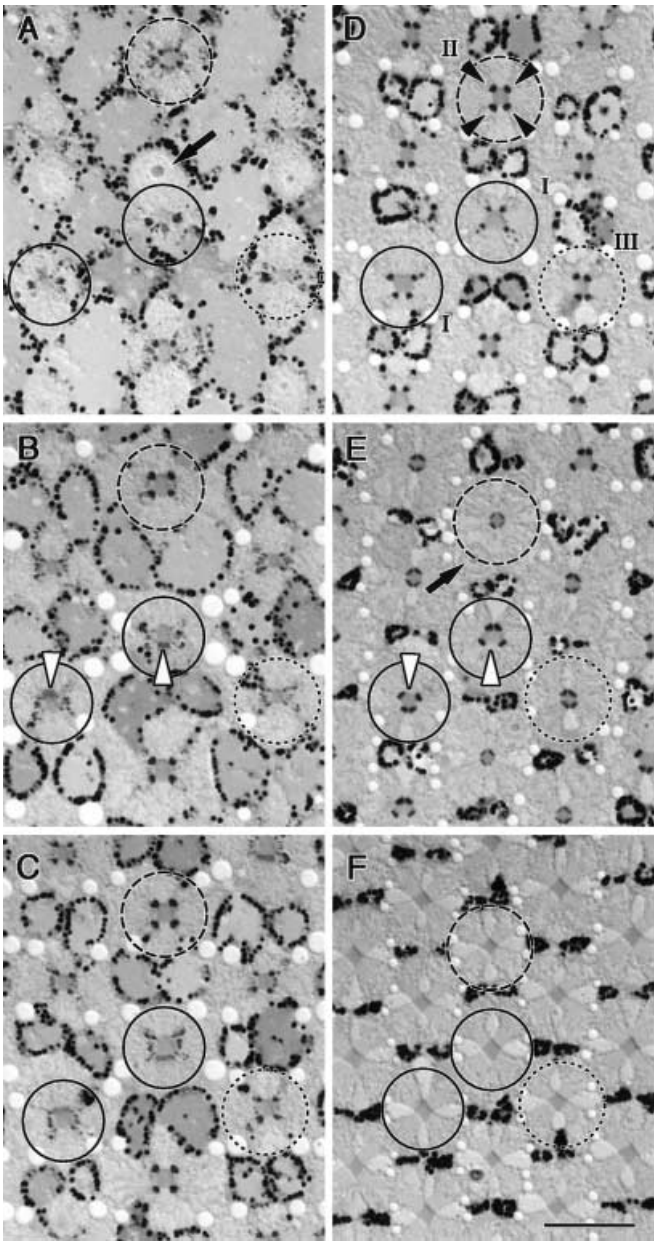

Fig. 5A–F Transverse sections of the same region of a *Pieris rapae* compound eye at different depths. *Circles* indicate identical sets of ommatidia. Depth: 140 µm (**A**), 180 µm (**B**), 220 µm (**C**), 260 µm (**D**), 300 µm (**E**), 360 µm (**F**). *Arrows* in **A** and **E** indicate nuclei of a distal and a proximal photoreceptor, respectively. *Roman numerals* attached to the *circles* in **D** indicate ommatidial types I (*solid circles*), II (*dashed circle*), and III (*dotted circle*). *Black arrowheads* in **D** indicate the perirhabdomeral pigment clusters. *White arrowheads* in **B** indicate low density pigmentation in a distal photoreceptor of type I ommatidia. *Bar* 10 µm

Rhabdom structure

We further investigated the structural differences between the ommatidial types by electron microscopy (summarized in Table 1). Figure 6 shows a set of electron micrographs of all three types of ommatidia sectioned at a depth of 140 µm (Fig. 6A, D, G), 240 µm (Fig. 6B, E, H), and 340 µm (Fig. 6C, F, I) from the corneal surface. We hereafter refer to these depths as distal, middle, and proximal, respectively.

In the distal region of type I ommatidia, the R2 photoreceptor bears straight microvilli parallel to the dorsoventral (vertical) axis of the animal (Fig. 6A). The R1 microvilli are parallel but not straight: they curve left or right depending on the depth as seen in Fig. 6A. This arrangement has been previously described (see Fig. 3c in Kolb 1978). The other distal photoreceptors, R3 and R4, bear straight microvilli parallel to the horizontal axis at this level (Fig. 6A). The cross-sectional area of the rhabdomere of R1 is larger than that of R2. The R3 and R4 rhabdomeres are even smaller. The proximal photoreceptors, R5–8, have no microvilli at this level. The low-density pigmentation in either R1 or R2 of type I ommatidia (Fig. 5B, white arrowhead) is seen in Fig. 6A as small pigment granules accumulated close to the rhabdom edge in an R2 photoreceptor. In the middle region of type I ommatidia, the R1 microvilli curve in two directions, whereas those of R2 are still straight (Fig. 6B). The microvilli of R3 and R4 curve in two directions. The area of the rhabdomere of R2 is larger than that of R1. The pigmentation in the middle region is prominent even in R5–8, although these photoreceptors bear only a few microvilli here. In the proximal region, R1 no longer has microvilli, whereas R2 still has a large rhabdomere with straight and vertically oriented microvilli. The microvilli of R5–8 are diagonally oriented and straight (Fig. 6C).

The rhabdomeres of R1–4 photoreceptors of type II ommatidia all bear microvilli that curve in two directions (Fig. 6D, E). The rhabdomeres are larger in R1 and R2 than in R3 and R4. The overall shape of the rhabdom in the distal region is square. The dense pigment clusters near the rhabdom are located in R5–8 photoreceptors (Fig. 6D). The rhabdom becomes round in the middle region (Fig. 6E). Here, R5–8 start to have microvilli. The pigmentation of R5–8 is still dense. Proximally, the microvilli of R1–4 completely disappear, and those of R5–8 form the rhabdom. The R5–8 microvilli are oriented diagonally (Fig. 6F).

The rhabdomeres of R1–4 of type III ommatidia all bear microvilli that curve in two directions (Fig. 6G–I). A sparse pigmentation is found in the cell body of R3–8 (Fig. 6G). In the middle region, R5–8 have a few short microvilli (Fig. 6H). The pigmentation in R5–8 becomes denser here.The pigment spots form a dorso-ventrally elongated rectangle because of the oval shape of the rhabdom (Fig. 6H). In the proximal region, the microvilli of R5–8 of type III ommatidia become longer (Fig. 6I).

Fig. 6 Electron micrographs of transverse sections of rhabdoms of type I (**A–C**), type II (**D–F**), and type III (**G–I**) ommatidia (*R* rhabdom). Depth: about 140 µm (**A, D, G**), 240 µm (**B, E, H**), and 340 µm (**C, F, I**). **J** Depth: about 400 µm (unidentified ommatidial type). **K** Longitudinal section of a rhabdom in the proximal region. **L** Transverse section at the basal region where R9 bears a few microvilli (*arrowheads*). *Numbers* in **E** and **L** refer to the photoreceptor number. *Bar* 1 µm ▶

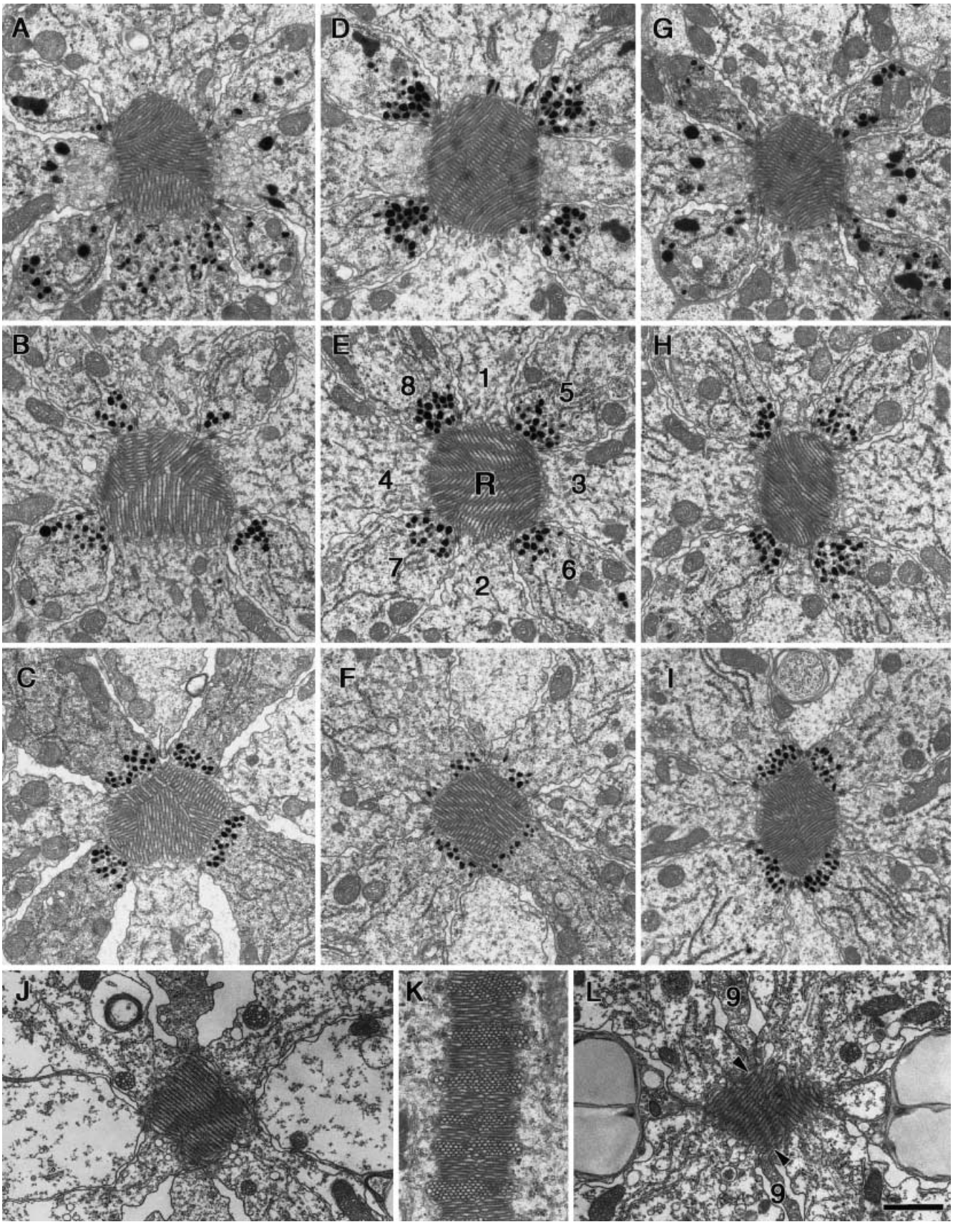
A
D
G
B
E
8
1
5
4
R
3
7
2
6
H
C
F
I
J
K
L
9
9

Table 1 Summary of the characteristics of the three ommatidial types in *Pieris* eyes

Type	Pigment clusters	Frequency (%)	Fluorescence	Reflection		Rhabdom structure, microvillar orientations of photoreceptors, rhabdomere length (start~end in μm)				
				610 nm	700 nm	R1	R2	R3/4	R5–8	R9
I	Trapezoid	49.5	–	+	–	Curved, two directions, 80~300	Straight, vertical, 130~380	Curved, two directions, 80~360	Straight, diagonal, 280~480	Straight, two directions 460~480
II	Square	28.8	+	–	+	Curved, two directions, 80~300		Curved, two directions, 80~300	Straight, diagonal, 240~480	
III	Rectangle	21.7	–	+	–	Curved, two directions, 80~300		Curved, two directions, 80~360	Straight, diagonal, 240~480	

Common to all three types is the disappearance of the pigmentation in R5–8 in the region close to the basement membrane (see Fig. 5F). At a depth of 420 μm from the corneal surface, all rhabdoms consist of the straight and diagonally oriented microvilli of R5–8 photoreceptors (Fig. 6J), forming an alternating banded organization (Fig. 6K) in the proximal one-third of the rhabdom. Figure 6J shows a layer where the microvilli of R6 and R8 occupy the whole rhabdom; R5 and R7 bear microvilli at layers slightly above and below this level (see also Meyer-Rochow 1971; Shimohigashi and Tominaga 1991). The basal photoreceptor R9 adds a few microvilli to the rhabdom close to the basement membrane (arrowheads in Fig. 6L).

Discussion

The ommatidia of *Pieris rapae* are divided into three classes based on their differences in pigmentation, fluorescence, reflection, and rhabdom ultrastructure. The characteristics of each ommatidial type is summarized in Table 1.

Pigmentation and tapetal reflection

The red eyeshine seen in the ventral eye region of the small white under epi-illumination with white light is attributable to a green-yellow reflecting tapetum in combination with a red-screening pigment filter (Ribi 1979a, 1979b, 1980). The observed red reflection is light that has been reflected by the tapetum and that has not been absorbed by the screening pigment lining the rhabdom during its propagation through the rhabdom. The diameter of the *Pieris* rhabdom is less than 2 μm, and when light propagates in such a thin light guide, a significant proportion of the light flux actually travels outside the rhabdom. This so-called boundary wave is partly absorbed by the red pigment, depending on its density. Short-wavelength light is strongly absorbed and long-wavelength (red) light passes predominantly unaffected. The function of the red pigment is to shift the sensitivity spectrum of photoreceptors in the proximal part of the ommatidia into the red (Ribi 1978), as also occurs in *Papilio* (Arikawa et al. 1999b).

We have found that the eyeshine is a mixture of pale-red and deep-red (Fig. 2) and emerges from two classes of ommatidia that have reflectance spectra peaking at about 635 and 675 nm, respectively (Fig. 3). As the long-wavelength limit of the spectra is determined by the tapetum, it follows from Fig. 3 that the two ommatidial classes must have different tapeta. The short-wavelength limit of the reflectance spectra is determined by the absorbance spectra of the screening pigment in the photoreceptors, and hence, it must be concluded that the two classes also have different screening pigments. Histology has underscored this conclusion (Fig. 4). In light-microscopic sections, the pigment of type II ommatidia appears as deep-red, whereas type I and III have a pale-red pigmentation (Fig. 5B). The deep-red pigmentation of type II ommatidia is apparently responsible for the low reflection below 630 nm light. The finding that type I and type III both reflect about maximally at 635 nm indicates that these two types are spectrally similar, at least with respect to the pigmentation and tapetal reflection. The functional consequences of the different combinations of tapetum and screening-pigment filters depend on the visual pigments in the photoreceptors that receive the filtered light. The spectral shifts induced by the pale-red and deep-red pigments will be distinctly different; these shifts will be augmented by the tapetal reflectors.

A fluorescent filter pigment?

Type II ommatidia fluoresce under UV and violet epi-illumination. The present evidence suggests that the fluorescence is attributable to a retinoid. In the *Papilio* retina, we have previously found a set of ommatidia fluorescing under UV epi-illumination, but not under violet epi-illumination. The origin of the UV-induced fluorescence is 3-hydroxyretinol. This retinoid functions as a UV-absorbing spectral filter, which changes UV receptors into violet receptors, having a very narrow sensitivity spectrum peaking at 400 nm (Arikawa et al. 1999a; Kitamoto et al. 2000). A retinol-binding protein, *Papilio* RBP, whose ligand is 3-hydroxyretinol, has recently been identified (Ozaki et al. 2000). *Pieris* eyes are now known also to contain a protein that fluoresces under UV

illumination and that is immunoreactive to the antibody against the *Papilio* RBP (Wakakuwa et al. 2001). Taken together, the UV-induced fluorescence of the *Pieris* ommatidia most likely originates from retinoid attached to an RBP. The retinoid probably functions as a spectral filter.

Rhabdom structure

Light- and electron-microscopic histology show that the ommatidia with the pale-red pigment must indeed be divided into two different types in view of the rhabdom structure and the arrangement of the pigment clusters adjacent to the rhabdom. This establishes that there are three types of ommatidia in the *Pieris* ventral eye region. In all three types of ommatidia, the rhabdomeres of the distal photoreceptors (R1–4) are not uniform. A clear feature of most distal photoreceptors is that the microvilli in a single photoreceptor curve into two directions. Such an arrangement should decrease the polarization sensitivity of the photoreceptors. Honeybee ommatidia in the ventral region of the compound eye are twisted; this probably eliminates undesirable polarization signals (Menzel 1975). *Pieris* ommatidia are not twisted, which is also the case in other butterflies (Arikawa and Uchiyama 1996; Kinoshita et al. 1997). Having curved microvilli is probably a butterfly strategy to counteract undesirable polarization sensitivity. Of course, polarization signals are not always undesirable (Rossel 1989; Perez et al. 1997). The distal photoreceptor in type I ommatidia (R1 or R2), which has a large rhabdomere with straight and parallel microvilli (Fig. 6A–C) should be useful for detecting polarization.

Perspectives

A striking characteristic of butterfly eyes is their ommatidial heterogeneity. What is its function? Our present hypothesis is that this heterogeneity is crucial for color vision. The three different types of ommatidia of *Papilio xuthus*, in which we first studied ommatidial heterogeneity in detail, contain different sets of spectral receptors that can be divided into at least five spectral types (Arikawa et al. 1987). Similarly, the compound eye of *Pieris rapae* is known to contain at least five different classes of spectral receptors (Shimohigashi and Tominaga 1991). The present anatomical study, showing that there are three anatomically distinct ommatidia, together with the different colors of the tapetal reflection observed in the different ommatidia, strongly indicates that each ommatidial type has a unique set of spectral receptors. Electrophysiological studies providing further evidence are presently under way.

Acknowledgements We thank Dr. Michiyo Kinoshita for discussion and technical advice. We also thank Dr. Justin Marshall for critically reading the manuscript and language editing.

References

Arikawa K, Stavenga DG (1997) Random array of colour filters in the eyes of butterflies. J Exp Biol 200:2501–2506

Arikawa K, Uchiyama H (1996) Red receptors dominate the proximal tier of the retina in the butterfly *Papilio xuthus*. J Comp Physiol [A] 178:55–61

Arikawa K, Inokuma K, Eguchi E (1987) Pentachromatic visual system in a butterfly. Naturwissenschaften 74:297–298

Arikawa K, Mizuno S, Scholten DGW, Kinoshita M, Seki T, Kitamoto J, Stavenga DG (1999a) An ultraviolet absorbing pigment causes a narrow-band violet receptor and a single-peaked green receptor in the eye of the butterfly *Papilio*. Vision Res 39:1–8

Arikawa K, Scholten DGS, Kinoshita M, Stavenga DG (1999b) Tuning of photoreceptor spectral sensitivities by red and yellow pigments in the butterfly *Papilio xuthus*. Zool Sci 16:17–24

Bernard GD, Miller WH (1970) What does antenna engineering have to do with insect eyes? IEEE Student J 8:2–8

Goulson D, Cory JS (1993) Flower constancy and learning in foraging preferences of the green-veined white butterfly *Pieris napi*. Ecol Entomol 18:315–320

Kandori I, Ohsaki N (1996) The learning abilities of the white cabbage butterfly, *Pieris rapae*, foraging for flowers. Res Popul Ecol 38:111–117

Kinoshita M, Sato M, Arikawa K (1997) Spectral receptors of nymphalid butterflies. Naturwissenschaften 84:199–201

Kinoshita M, Shimada N, Arikawa K (1999) Colour vision of the foraging swallowtail butterfly *Papilio xuthus*. J Exp Biol 202:95–102

Kitamoto J, Ozaki K, Arikawa K (2000) Ultraviolet and violet receptors express identical mRNA encoding an ultraviolet-absorbing opsin: identification and histological localization of two mRNAs encoding short-wavelength-absorbing opsins in the retina of the butterfly *Papilio xuthus*. J Exp Biol 203:2887–2894

Kolb G (1978) Zur Rhabdomstruktur des Auges von *Pieris brassicae* L. (Insecta, Lepidoptera). Zoomorphologie 91:191–200

Menzel R (1975) Polarization sensitivity in insects with fused rhabdoms. In: Snyder AW, Menzel R (eds) Photoreceptor optics. Springer, Berlin Heidelberg New York, pp 372–387

Meyer-Rochow VB (1971) A crustacean-like organization of insect-rhabdoms. Cytobiologie 4:241–249

Obara Y, Hidaka T (1968) Recognition of the female by the male, on the basis of ultra-violet reflection, in the white cabbage butterfly, *Pieris rapae crucivora* Boisduval. Proc Jpn Acad 44:829–832

Ozaki K, Wakakuwa M, Arikawa K, Kawamura S (2000) Identification of a novel retinol-binding protein in the eye of the butterfly, *Papilio xuthus*. Zool Sci 17S:98

Perez SM, Taylor OR, Jander R (1997) A sun compass in monarch butterflies. Nature 387:29

Ribi WA (1978) Ultrastructure and migration of screening pigments in the retina of *Pieris rapae* L. (Lepidoptera, Pieridae). Cell Tissue Res 191:57–73

Ribi WA (1979a) Coloured screening pigments cause red eye glow hue in Pierid butterflies. J Comp Physiol [A] 132:1–9

Ribi WA (1979b) Structural differences in the tracheal tapetum of diurnal butterflies. Z Naturforsch 34c:284–287

Ribi WA (1980) The phenomenon of eye glow. Endeavour 5:2–8

Rossel S (1989) Polarization sensitivity in compound eyes. In: Stavenga DG, Hardie RC (eds) Facets of vision. Springer, Berlin Heidelberg New York, pp 298–316

Scherer C, Kolb G (1987) Behavioral experiments on the visual processing of color stimuli in *Pieris brassicae* L. (Lepidoptera). J Comp Physiol [A] 160:645–656

Shimohigashi M, Tominaga Y (1991) Identification of UV, green and red receptors, and their projection to lamina in the cabbage butterfly, *Pieris rapae*. Cell Tissue Res 263:49–59

Stavenga DG (2002) Reflections on colourful ommatidia of butterfly eyes. J Exp Biol (in press)

Stavenga DG, Kinoshita M, Yang E-C, Arikawa K. (2001) Retinal regionalization and heterogeneity of butterfly eyes. Naturwissenschaften 88:477–481

Wakakuwa M, Ozaki K, Arikawa K (2001) Localization and function of the retinol-binding protein in the butterfly eyes. Zool Sci 185:101